STOMAGEN-like Regulates Stomatal Generation Causing Increased Water Use Efficiency during C_4 Evolution

Yong-Yao Zhao[1,2], Amy Mingju Lyu, Genyun Chen, Xin-Guang Zhu[1,2]

1. Center of Excellence for Molecular Plant Sciences, Chinese Academy of Sciences

2. State Key Laboratory for Plant Molecular Genetics

Abstract

Compared with C_3 plants, C_4 plants maintain lower stomatal conductance (g_s), attributed to decreased maximal stomatal conductance (g_{smax}), without losing photosynthetic CO_2 uptake rate. Which stomatal characteristics caused the decreased g_{smax} and how did the characteristics change along C_4 evolution as well as the molecular mechanism underlying this change remains unknown.

Stomatal patternings were examined in *Flaveria* genus, which contains species at different evolutionary stages from C_3 to C_4 photosynthesis. We further used comparative transcriptomics, transgenic experiments and semi-*in-vitro* analysis to identify the gene underlying the decreased g_{smax} in C_4 species.

Results were as follows: the evolution from C_3 to C_4 species was accompanied by a stepwise decrease in stomatal density (*SD*) and dramatic decreased *SD* occurred between C_3-C_4 species and C_4-like species; *FSTOMAGEN* gene positively controls *SD* and its changed expression underlies the decreased *SD* during C_4 evolution; Furthermore, this mechanism is shared between monocotyledons and dicotyledons, indicated by the lower expression of *FSTOMAGEN* homologs in maize than rice.

This study suggests that lower *SD* is another major feature of C_4 evolution, besides C_4 enzymes and Kranz anatomy. *FSTOMAGEN* can be used to engineer lowered SD, a C_4 feature required in the current effort of C_4 crop engineering.

Key words:

Water use efficiency, Stomatal density, C_4 photosynthesis, STOMAGEN, Stomatal conductance

Introduction

Compared with C_3 plants, C_4 plants have higher light use efficiency (LUE) as a result of a CO_2 concentrating mechanism (*1*). At the same time, C_4 plants also have higher water use efficiency (WUE), as a result of both lower g_s and higher photosynthetic CO_2 uptake rate (A) due to the CO_2 concentrating mechanism (*2*, *3*). C_4 photosynthesis therefore optimizes water and carbon relations by reducing transpiration without compromising carbon assimilation (*4*). Improvements in WUE enables C_4 plants to better adapt to saline lands, hot and drought subtropical environments and open habitats compared with their close C_3 relatives, which raises the possibility that C_4 photosynthesis might have been selected as a water-conserving mechanism (*4*) and that water limitation might be the primary driver for the initial ecological advantage of C_4 over C_3 (*5-7*). Given that C_4 plants have higher photosynthetic energy conversion efficiency and higher potential for biomass productivity, their lower g_s is critical for the survival and fitness of C_4 plants in the field, especially in a world where water shortage is predicted to occur more often.

C_3 plants, *e.g.* eucalyptus and arabidopsis, can gain improved WUE through reducing transpiration under long-term changed environmental conditions by decreasing g_{smax} (*8*, *9*), which implies that the decreasing g_{smax} may be an option that plants use to increase WUE. Indeed, phylogenetically informed comparison shows that C_4 plants usually have a lower g_{smax} compared with their close C_3 relatives (*10*), indicating that the lower g_{smax} contribute to the higher WUE of C_4 land plants.

Therefore, low g_{smax}, same as the C_4 metabolite shuttle and Kranz anatomy, may be a required feature for C_4 land plants. But so far, in comparison with the extensive studies on the C_4 metabolite shuttle and Kranz anatomy, relatively little effort has been invested into studying the mechanism underlying the decreased g_{smax} in C_4 plants.

In principle, g_{smax} positively correlates to operating g_s (*8*) and the g_{smax} is determined by stomatal density (*SD*) and stomatal size (*SS*). In Eucalyptus and Arabidopsis, *SD* positively controls g_{smax} and operating g_s (*8, 11-13*). Higher *SD* also appears to have been selected as a strategy to gain higher g_{smax} to cope with low atmospheric CO_2 levels over the last 400 million years (*14*). In contrast, when grown under drought, potato plants severely reduce *SS* to lower operating g_s and increase WUE (*15*). Under ABA treatment, a sufficiently small *SS* can lower g_{smax} to achieve higher WUE in *Tradescantia virginiana (16)*. Therefore, in different species or under different environmental conditions, either *SD* or *SS* is used as a primary determinant for g_{smax} in plants. In the case of C_4 photosynthesis, it also remains unknown whether SD or SS is the dominant characteristic responsible for the lower g_{smax} in C_4 relative to C_3 plants. For example lower g_{smax} of different species in one C_4 clade were attributed to either smaller *SS* or lower *SD* (*10*), which may be a result of a compounded phylogenetic effect, i.e. species used in the study were evolutionarily distant from each other and hence genetic factors unrelated to photosynthesis may influenced stomatal patterning (*10*).

Stomatal development is controlled by a well-studied developmental patterning program (*17, 18*). Stomatal patterning is controlled by a series of ligands and the transmembrane receptors, leading to downstream changes of MAPKK, MAPKs and transcription factors, ultimately influencing stomatal development (*17, 18*). TOO MANY MOUTHS (TMM) and ERECTA-family (ERfs: ER, ERL1, ERL2) are receptor-like kinases that negatively regulate stomatal development (*19, 20*), and the TMM interacts with ERfs to regulate stomatal differentiation (*19, 21*). The ligands that binds to ER and TMM receptors are mainly EPIDERMAL PATTERNING

FACTOR/EPIDERMAL PATTERNING FACTOR-LIKE family (EPF/EPFL-family) petides, including EPF1, EPF2, and *STOMAGEN*/EPFL9 (*22*). The *EPF*/*EPFL*-family genes encode cysteine-rich peptides, which can fold into a three-dimensional structure through disulfide bond to drive stomatal patterning (*23*). Overexpression of *EPF1* decreases the number of stomata, whose loss of function mutation increases the number of stomata and results in stomatal cluster (*24*). *EPF2*, which acts earlier in stomatal development relative to *EPF1*, has a similar genetic effect as *EPF1* (*25*). *STOMAGEN*, in contrast to either *EPF1* or *EPF2*, positively regulates *SD* (*26-28*). *STOMAGEN* can compete with EPF1 and EPF2 for ERfs (*29*), and then prevent the phosphorylation of downstream receptors, which further results in the changed expression of three transcription factors of basic Helix-loop-Helix (bHLH) paralogs, SPCH, MUTE and FAMA, ultimately influencing stomatal development (*30*).

To study whether *SD* or *SS* underlies the decreased g_{smax} in C_4 species, here we use the *Flaveria* genus, a representative of dicotyledons which contains closely related species at different evolutionary stages from C_3 to C_4 photosynthesis. Using a genus with multiple intermediate species will enable examination of changes in stomatal patterning during C_4 evolution. In addition, rice and maize, as representatives of monocotyledons, are used to test whether the identified mechanism is conserved in monocotyledons as well. This study aims to answer the following questions: 1) Which stomatal patterning parameter, i.e. *SD* and *SS*, underlies the decreased g_{smax} in C_4 evolution and how did it change during the evolution? 2) What's the molecular mechanism underlying the change of this stomatal patterning parameter? 3) Is this molecular mechanism conserved between monocotyledons and dicotyledons?

Result

C_4 species reduce stomatal densities during C_4 evolution

The maximum value of operational g_s (marked with circles on figure) at saturated light intensity of C_3 *Flaveria* species is higher than C_4 species, indicating that the C_3 *Flaveria* species tends to have a higher g_s (Fig 1a). On the whole, the operational g_s at the saturated light of C_3 species and C_3-C_4 species in *Flaveria* are higher than C_4 species and C_4-like species (Fig 1b). We then compared the *SD* of different *Flaveria* species grown either outdoors or in greenhouse on both sides of leaves. We found that, in comparison to C_4 and C_4-like photosynthesis, the *SD* of C_3 and C_3-C_4 photosynthesis on the abaxial leaf surface of *Flaveria* were nearly 150% higher (Fig. 1d and e). With the progression from C_3 to C_4 species, there was a distinctly gradual decrease in *SD* (Fig. 1f and g). The difference in *SD* between C_3 and C_3-C_4 (type I) species wasn't as great as that between C_3 and C_4 species; and the *SD* of C_3-C_4 (type II) species fell in between C_3-C_4 (type I) and C_4-like species (Fig. 1d, e, f and g). The *SD* of C_4 and C_4-like species were similar, although $C_{4\text{-like}}$ is slightly smaller than C_4 (Fig. 1d, e, f and g). The g_s at saturated light of *F. sonorensis* (son) (C_3-C_4 (type I)) is extremely high (marked with circle on figure), matching with its highest *SD* within *Flaveria* genus (Fig 1a, f). The observed reductions in both g_s and *SD* of C_4 and C_4-like *Flaveria* species compared to C_3 and C_3-C_4 species suggest that the decrease in *SD* contributes most of the decrease in g_s during C_4 evolution (Fig 1h). For the adaxial leaf surface, the *SD* of C_3 species was again higher than that of the C_4 species, although the difference between *SD* in the intermediate species was less significant (Supplementary fig. 2a, b, c, d).

We next chose three *Flaveria* species, i.e. *F.robusta (rob)*, *F. ramosissima* (*ram*) and *F.bidentis (bid)* to represent C_3, C_3-C_4 and C_4 species, respectively, to conduct detailed analysis of gas exchange and guard cell morphological features. Similar to the saturated light condition, the WUE (A/g_s) of *rob* measured under unsaturated light intensity was also higher than *bid* (Fig.1c). Furthermore, under unsaturated light, the operational g_s of C_3 *Flaveria* species was 71% higher than that of C_4 species (Fig. 1c), consistent with the higher *SD* of C_3 species, implying that operational g_s under unsaturated light is also associated with *SD*. For plants grown in outdoor conditions,

SS which for this study was taken as guard cell length (*l*) showed the opposite trend. The *l* of *bid* was the longest (Fig. 1j). This inverse relationship between *SD* and *SS* was also observed earlier (*8, 10, 14*). In greenhouse, *l* of *ram* was the longest, however, *l* of *bid* and *rob* were almost the same, even though the *l* of *bid* was slightly longer (Fig. 1j). The ratio between the number of guard cells and the number of epidermal cells, i.e. the stomatal index (*SI*), in *rob* were both nearly 50% higher than *bid* and *ram* in plants grown in either greenhouse or outdoors, suggesting that the proportion of stomata occupying the epidermis, i.e. *SI*, contributed to the highest *SD* in rob (Fig. 1i and k). In addition to the above analysis of *Flaveria* plants grown from cuttings, we also planted *Flaveria* germinated from seeds. Results showed that the *SD* of C_3 species was again higher than C_4 species, consistent with the cuttings (Supplementary fig. 3).

FSTOMAGEN **positively controls stomatal density (*SD*) and may be a factor contributing to the decreased *SD* in C_4 *Flaveria* species**

The signaling pathway for stomatal development has been studied extensively, which includes a signal transduction, MAPK cascade and activation/inactivation of basic Helix-loop-Helix (bHLH) transcription factors (*17*). We first identified amino acid sequence encoded by homologs of stomatal development related genes in *Flaveria*. Amino acid sequence alignment analysis shows that homologs of epidermal patterning factor/epidermal patterning factor-Like gene family (*EPF*/*EPFL*-family) was conserved at the C-terminal part of amino acid sequence (Fig 2A, Supplementary fig 4). Each member of *EPF*/*EPFL*-family genes encodes a secretory protein containing a signal peptides at the N-terminus and a functional domain at the C-terminus (*24, 25, 31*). Analysis showed hydrophobicity of the homologs of EPFs/EPFL in *Flaveria* was similar to the EPF/EPFL, implying the homologs are also the secretory proteins and may have the same physiological function as EPF/EPFL (Supplementary fig 5). We hypothesized that either the amino acid sequence or

165 expression levels of stomatal developmental related genes changed during C_3 to C_4
166 evolution. Analysis results revealed no differences within the functional region of
167 amino acid sequence for STOMAGEN, EPF1 and EPF2 homologs between C_3 and C_4
168 species (Fig. 3d and supplementary fig. 4a, b), indicating the change of amino acid
169 sequence is unlikely to be a cause of the changed *SD* during C_4 evolution.

170 As an increased transcript abundance has been a major feature for many genes
171 related to C_4 cycle or transporters during C_3 to C_4 evolution in *Flaveria* **(*32, 33*)**, we
172 further compared the transcript abundance of these stomatal developmental related
173 genes between C_3 and C_4 species in *Flaveria* genus. The expression patterns of known
174 C_4 related genes in our data analysis were same as the multiple previous works, which
175 indicates that our data collection and analysis procedure were reliable (Supplementary
176 fig. 10) (*32*, *33*). First, we found that most homologs of stomatal developmental
177 related genes showed much higher transcript abundance in developing tissues as
178 compared to developed tissues (Fig. 3b), which is consistent with their function of
179 regulating stomatal differentiation in developing leaf (*24*, *26*, *28*, *34*). *STOMAGEN*,
180 *EPF1*, *EPF2* and *TMM* showed higher expression levels in C_3 species than in those in
181 C_4 species (Fig. 3b, Supplementary fig. 7). RT-qPCR quantification of the expression
182 levels of *STOMAGEN*, *EPF1*, *EPF2* homologs between C_3 and C_4 species also
183 confirmed the results from RNA-SEQ (Fig. 3c). Considering that the *EPF1*, *EPF2*
184 and *TMM* are negative regulators for stomatal development (*22*, *24*, *25*, *29*) and the
185 lower *SD* of C_4 species, these genes should not be the factors responsible for the
186 decreased *SD* in C_4 species. *STOMAGEN* is a positive regulator of *SD* (*22*, *26*, *27*),
187 whose lower expression in C_4 species was consistent with the decreased *SD* in C_4
188 species (Fig. 1d,e,f,g, Supplementary fig 3), and the expression of the reduced parts of
189 *STOMAGEN* was higher than that of *EPF1* and *EPF2*. In this study, we renamed
190 *STOMAGEN* in *Flaveria* as *FSTOMAGEN*.

191 There are considerable species differences in amino acid sequence of signal
192 peptide of *STOMAGEN* homologs, especially between species with large evolutionary
193 distance (Fig. 2a). The functional domain of *STOMAGEN* is however highly

194 conserved, not only between different *Flaveria* species (Fig. 3d), but also between
195 species that have a large evolutionary distance (Fig. 2a). In Arabidopsis, the increased
196 expression of *STOMAGEN* leads to increased *SD*, and when applied exogenously the
197 signal peptide is not required for synthetic *STOMAGEN* to induce the increased in *SD*
198 (*26, 27, 31, 34*), indicating the replacement of signal peptide will not affect the
199 *STOMAGEN*'s function increasing *SD*. A phylogenic tree constructed for *STOMAGEN*
200 from different plants can be divided into two clades, i.e. dicotyledon (blue clades) and
201 monocotyledon (red clades) (Fig. 2b). Previous studies showed that overexpressing of
202 either of the two rice homologs of *STOMAGEN* in rice can cause an increased *SD* in
203 Arabidopsis (*35, 36*), implying strong conservation of *STOMAGEN* function across
204 monocots and dicots. When plants are grown under environmental conditions that
205 promote or inhibit stomatal development e.g. at high or low light intensity, the
206 expression of *STOMAGEN* is known to increase or decrease, respectively (*12, 34, 37*).
207 A similar modulation of *STOMAGEN* expression levels was observed for rob when
208 grown at different light conditions (Supplementary fig 8).

209 In order to confirm that *FSTOMAGEN* can induce stomatal generation, we
210 overexpressed the *FSTOMAGEN* in *Arabidopsis*. We recombined the signal peptide of
211 *STOMAGEN* from *Arabidopsis* to the functional region of *FSTOMAGEN* and named
212 the hybrid gene as AFSTO (Fig, 2c). Overexpressing either the AFSTO or the intact
213 *FSTOMAGEN* (FSTO) from *F.robusta* into *Arabidopsis* resulted in increased *SD* (Fig.
214 2d, e, f); Furthermore, overexpression of *FSTOMAGEN* also induced clustered
215 stomata (Fig. 2e, f), as also reported for other *STOMAGEN* homologs (*26*). To further
216 confirm that *FSTOMAGEN* can increase *SD* in *Flaveria*, we synthesized a peptide
217 representing the F*STOMAGEN* functional region, consisting of 45 amino acids (Fig.
218 2a). *In vitro* application of the F*STOMAGEN* peptide increased the *SD* and caused
219 stomatal cluster in *F. bidentis*, and the amount of F*STOMAGEN* is positively
220 correlated with the number of stomata as previously reported (*26, 27, 31, 34, 35*) (Fig.
221 2g, h, i, supplementary fig. 12). These results demonstrate that, in addition to its *in*
222 *vivo* function, *in vitro* application of F*STOMAGEN* can also directly positively

223 regulate *SD* in *Flaveria*. This is consistent with the notion that *STOMAGEN* is
224 expressed in mesophyll cells and is secreted out of cells to influence the stomatal
225 development in the epidermal layer in *Arabidopsis* (*26*, *27*).

226

227 **The low transcript abundance of *FSTOMAGEN* underlie the decreased stomatal**
228 **density of *Flaveria* species during C_4 evolution**

229 We examined the copy number of *STOMAGEN* in *Flaveria* species using blastn
230 with the coding sequence of *FSTOMAGEN* as query sequence against all the
231 assembled contigs in each *Flaveria* species. Results show that there was only one hit
232 sequence with e-value less than 10^{-5} in each species, suggesting that there is a single
233 copy of *FSTOMAGEN* in each *Flaveria* species (Supplementary fig. 11). Therefore
234 we can ignore the impact of other *FSTOMAGEN* paralogs on stomatal development,
235 and there will be no quantitative errors in the gene expression levels caused by other
236 paralogs not being considered. Further examination of the RNA-seq data of *Flaveria*
237 showed that the expression levels of *FSTOMAGEN* in C_3 species were markedly
238 higher than those in C_4 species along different developmental stages of leaves (Fig.
239 3e). During leaf growth and development, the expression of *FSTOMAGEN* in both *bid*
240 and *rob* increased first, reaching the highest level at leaf development stage 3 or 4,
241 and then declined (Fig. 3e). These similar patterns of *STOMAGEN* expression in these
242 two *flaveria* species indicated that it would be valid to compare the *STOMAGEN*
243 expression levels in leaves at the same development stage between different *Flaveria*
244 species. The expression levels of *FSTOMAGEN* in C_4 and C_4-like species were lower
245 than those in C_3 and C_3-C_4 species in *Flaveria* based on either RNA-seq or RT-qPCR
246 quantification (Fig. 3b, f, g), consistent with the different *SD* among different
247 photosynthetic types (Fig. 1d, e). Expression levels of *FSTOMAGEN* increased with
248 the increase of *SD* when the data from a large number of *Flaveria* species with
249 different photosynthetic type were combined (Fig. 3h). Together these results suggest

that a gradual change in the *FSTOMAGEN* expression levels underlied the stepwise change in *SD* during C_4 evolution.

The role of *FSTOMAGEN* homologs in regulating SD between rice and maize.

Species of the *Flaveria* genus are dicotyledonous plants. To gain further insight into whether *STOMAGEN* might be a generic factor leading to the difference in *SD* between C_3 and C_4 species across higher plants, we tested whether *STOMAGEN* homologs are differentially expressed between C_3 and C_4 species in monocotyledon species. We used rice and maize in this study. The abaxial leaf *SD* of C_3 rice were 240% higher than that of C_4 maize, consistent with a 574% higher g_s in rice compared to maize (Fig. 4a, b). The stomatal length (*l*) in maize was 133% longer, and stomatal index (*SI*) showed significant difference (Fig. 4a, b). *SD* showed a positive relationship with *STOMAGEN* transcript levels in Arabidopsis, rice and maize (Fig. 4e, f), i.e. with the increase in the transcript abundance of *STOMAGEN* homologs, the *SD* gradually increases. We did not observe a significant difference in the efficacy of *STOMAGEN* homologs from Arabidopsis and either rice or maize in terms of their effectiveness in controlling *SD* (Fig. 4e,f), suggesting that the function of *STOMAGEN* homologs is highly conserved between dicotyledonous and monocotyledonous plants. This similarity in efficacy allowed us to compare the expression levels of *STOMAGEN* homologs from different species, even though their amino acid sequences differ. To test whether the difference in *SD* between rice and maize is due to changed expression levels of *STOMAGEN*, we combined the transcript abundance of their different paralogs, since there are two and three paralogs of *STOMAGEN* in rice and maize (*35*), respectively. We found that *STOMAGEN* homologs in rice had much higher transcript abundance than that in maize (Fig. 4d), while the transcript abundance of other stomatal development related genes did not differ to the same extent between rice and maize (Fig. 4c). Together our observations

277 suggest that the lower transcript abundance of *STOMAGEN* homologs in maize also
278 underlies its lower *SD* compared with rice.

279

280 **Method**

281 **Plant materials, sample condition and data sources**

282 All *Flaveria* species used in this study were kindly provided by Prof. Rowan F.
283 Sage (University of Toronto). Plants used for stomatal phenotyping were re-grown
284 from cuttings. Placed in an environment humidified with humidifiers to generate roots.
285 After plants generated roots, they were transferred outdoors (Institute of Plant
286 Physiology and Ecology, Chinese Academy of Sciences, Shanghai, China), and
287 transplanted into 4-L pots filled with topsoil in April. In July, the number of stomata
288 on abaxial and adaxial surfaces of leaves were counted. Another batch of *Flaveria*,
289 which were also grown from cuttings, were transferred to the phytotron (Institute of
290 Plant Physiology and Ecology, Chinese Academy of Sciences, Shanghai, China).
291 Growth temperature of the phytotron was maintained at 25-28□, photoperiod was
292 maintained at 16h light / 8h dark, relative humidity (RH) was at 60-65% and
293 photosynthetic photon flux density (PPFD) was maintained at about 180 μmol m^{-2} s^{-1}.
294 Two months later, the numbers of stomata on the abaxial and adaxial surfaces of
295 leaves were counted. RNA was extracted from 1.5~3.0 cm long young leaves on the
296 axial shoot which were still expanding. Three hours before sampling, we provided
297 sufficient water to ensure that plants were not water limited, since drought and water
298 status can affect expression levels of *STOMAGEN* and SD (*12*, *38*). Gene expression
299 was further examined under normal growth conditions by RT-qPCR for the *F.robusta*,
300 *F.rammosissima* and *F.bidentist*, which are representative of C_3, C_3-C_4, C_4 species in
301 the *Flaveria* genus. These three species were grown in the same phytotron with the
302 same environmental conditions, except that we did not water plants before sampling.
303 To test whether plants grown from cuttings or from seeds show difference in the *SD*,
304 we further grew *Flaveria* species from seeds in phytotron and examined stomatal

properties. Same environmental conditions were maintained for phytotron as above. Two months after germination of seeds, we counted stomatal number.

All plants were well watered to avoid drought stress during their growth. We supplied the same amount of commercial nutrient solution (Peters Professional, SCOTTS, N:P:K = 20:20:20+TE, at recommended dose for application) to the different species to avoid nutrient deficiency.

Rice (*Oryza Sativa Nipponbare*) and maize (*Zea maize* B73) were grown in the greenhouse (Institute of Plant Physiology and Ecology, Chinese Academy of Sciences, Shanghai, China) under a PPFD of 550 umol/m^2/sec, a photoperiod of 12h light / 12h dark, and a daytime temperature of around 31℃ and a night-time temperature of around 22℃. The RH was maintained at around 50-55%. The plants were regularly watered to avoid drought stress.

In addition to the expression data collected by in this study, we also used public data for comparison of transcript abundance. Considering that stomatal development related genes are mainly expressed in young tissues, in each of these used public data source, only samples for young leaves or young tissue of leaves were included. The transcript levels of stomatal development related genes in *Flaveria* were obtained from three studies. The first data source is the One Thousand Plants (1KP) Consortium; we subsequently analyzed the data according to the methods described in previous work (*39, 40*). The second and third data sources were Mallman et al (2014) (*33*) and Kumari Billakurthi et al (2018) (*41*), respectively. For the second data source, the second and fourth visible leaves were sampled; the second leaf was not completely mature, and stomatal developmental related genes were still actively expressed. Expression levels for stomatal development related genes in developing leaves for rice and maize were obtained from Wang et al. (*42*).

Conservation and hydrophobicity analysis of proteins

Amino acid sequence of the homologs of *STOMAGEN*, EPF1 and EPF2 were aligned by clustalx, and graphs for the multiple alignments were drawn with ESPrit 3.0 (*43*) (http://espript.ibcp.fr/ESPript/cgi-bin/ESPript.cgi). Hydrophobicity of proteins was determined by ProtScale (*44*) (https://web.expasy.org/protscale/).

Construction of the phylogenetic tree of *STOMAGEN*

To construct the phylogenetic tree of *STOMAGEN*, we queried the orthologs of *STOMAGEN* in representative species in Viridisplantae. Protein sequence of *STOMAGEN* from *A. thaliana* (AT4G12970) was used as query sequence. We selected 29 representative species which were chosen according to two criteria: 1) one species to represent each main lineage, e.g., M.pusilla represents M.pusilla chlorophyte, and M.polymorpha represents the ancestral type of Embryophyte; 2) one lineage to represent monocot and one lineages to represent dicot. We used the brassicaceae family (including *Arabidopsis thaliana*) to represent dicot and used the grass family (including *Oryza sative*) to represent monocot. The protein sequences of representative species were downloaded from Phytozome (https://phytozome.jgi.doe.gov/). Protein sequences for the *Flaveria* species were predicted using OrfPredictor (*45*) based on denovo assembled transcript as described in (*46*). *STOMAGEN* orthologs in *Flaveria* and other species (except for *A. thaliana*) were predicted by using blastp from BLAST (V 2.2.31+) (*47*) with a E-value threshold of 1e-5, where the protein sequence of STOMAGEN from *A. thaliana* was used as query. Protein sequences of *STOMAGEN* orthologs were then aligned using MUSCLE (*48*). Phylogenetic tree was constructed by applying Raxml (*49*) based on protein sequences using PROTGAMMAILG (General time reversible amino acid substitution model with assumption that variations in sites follow gamma distribution) model. Bootstrap scores were obtained based on 100,000 bootstraps.

Measurement of stomatal conductance (g_s)

The LI-6400 Portable Photosynthesis System (Li-Cor, Inc., Lincoln, NE, USA) was used to measure g_s on the youngest fully expanded leaves from approximately three-months-old *Flaveria* plants grown from cuttings. During the measurements, the cuvette temperature was maintained at 25□, the PPFD in the cuvette was maintained at ~500 µmol/m²s and the CO_2 concentration was maintained at around 400 ppm. Chamber humidity was matched to ambient air humidity. Leaf-to-air vapor pressure difference (VPD) was maintained around 1.1 kPa. Before the g_s measurements, *Flaveria* plants were adequately watered, maintained under constant light with a PPFD of ~500 umol/m^2s until g_s reached a steady state. Six different plants were used to measure g_s for every *Flaveria* species. Eight different plants were used to measure g_s for both rice and maize. External environments during the g_s measurements for rice and maize were controlled to be their growth conditions. We used the third or fourth leaves from the apex for g_s measurements. In maize and rice, the16-day-old third leaves. which were the youngest mature leaves, were used for gas exchange measurements (*42*).

Phenotyping stomatal traits

The youngest fully expanded leaves (usually the third or fourth leaves from the apex) at the main stem were used to phenotype stomata related traits. In *Flaveria and maize*, stomata related traits were observed using both nail polish method and epidermis directly peeled from leaves (*6, 11*). For the first method, nail polish was painted on the both leaf surfaces to produce the impressions of epidermis. After drying of the nail polish, the nail polish was peeled off the leaf and placed on a microscope slide for examination. For the second method, leaf epidermis was peeled off manually and transferred onto microscope slide. For the measurement of SI in rice, a small piece of rice blade was soaked in 9:1 (V/V) ethanol:acetic acid overnight, washed with water and cleared in chloral hydrate solution (glycerol:chloral

hydrate:water, 1:8:1) overnight, and then placed on a microscope slide for imaging. Light microscope (smarte; CNOPTEC), camera and image processed software (OPTPRO; CNOPTEC) were used to observe and image epidermis at x100 magnification. Center of a leaf was chosen to count and measure stomatal density and stomatal length respectively. Five stomata randomly chosen along a diagonal of the varnish peels or epidermis were measured for stomatal length.

RNA isolation and quantitative real-time PCR

The leaf samples taken from main stem were immediately frozen in liquid nitrogen and used directly for RNA extraction. Total RNA was extract from the young leaves using the PureLink RNA Mini kit (Thermo Fisher Scientifc). First-strand cDNA was synthesized by the TransScript One-step gDNA Removal and cDNA Synthesis SuperMix (TRANSGEN). Real-time PCR was performed on the CFX connect^{TM} (Bio-Rad) using the UNICON^{TM} qPCR SYBR ®Green Master Mix (YEASEN) according to the manufacturer's instructions. The calculation of expression according to the $2^{-\Delta\Delta CT}$.

The expression stability of internal reference genes was assessed by the software: geNORM and NormFinder (*50*, *51*). Specifically, we first calculated the coefficient of variations (CV) of all genes in different *Flaveria* species. After that, all genes were sorted according to the calculated CV values. 150 genes with the lowest CV were selected as potential candidate reference genes. Among these, those with mean expression level >300 were chosen as candidate reference genes. We also included those commonly used house-keeping genes, which include *UBC9* (AT4G27960), *UBQ11* (AT4G05050), *ACT7* (AT5G09810), *GAPDH* (AT1G13440), *EF1a* (AT5G60390), *CACMS* (AT5G46630) (Supplementary fig. 6a, b, d), as the internal reference genes in this study. The specificity of the primers (Supplementary table 2) for all these candidate reference genes were identified by agarose electrophoresis (Supplementary fig. 6c). With Genorm (Supplementary fig. 6e) and Normfinder

(Supplementary fig. 6f), we concluded that *ACT7*, *EF1a* and *HEME2* showed stable expression levels across rob, ram and bid. *EF1a* and *ACT7* are classic reference genes, and they showed minor variations under different conditions. The geometrical means of the expression level of *ACT7* and *EF1a* were finally used as normalization factors. All primers used for RT-qPCR are listed in Supplementary table 2. For each gene, three technical replicates and at least three biological replicates were performed.

Vector construction and transformation

A list of primer sequences were used for plasmid construction (Supplementary table 2). The *STOMAGEN* and *FSTOMAGEN* DNA sequences, named ATSTO-cDNA and FloSTO-cDNA respectively, were PCR-amplified from cDNA in Arabidopsis and *F.robusta*. To obtain the AFSTO fragment, signal peptide region of *STOMAGEN* was cloned from ATSTO-cDNA by PCR-amplification, and functional region of *FSTOMAGEN* was PCR-amplified from FloSTO-cDNA. The signal peptide and functional region were combined by fusion PCR. To obtain an intact *FSTOMAGEN* (FSTO) gene, the whole gene in *F.robusta*, including signal peptide, propeptide and *STOMAGEN* functional region, was amplified from the cDNA of F.robusta. To over-express AFSTO and FSTO, the AFSTO and FSTO were cloned separately to a pcambia-3300 binary vector which has a CaMV 35S promoter. This construct was introduced into *A. tumefaciens* strain GV3101, transformed into Arabidopsis using a floral dipping procedure. Transgenic lines were selected on soil that had been treated with a diluted solution of phosphinothricin (diluted 3000 times) over night. Phenotype was observed using three individual leaves for each line, and we used three lines of T1 plant in total.

Refolding of synthetic *FSTOMAGEN*

Chemically synthesized peptide (Synthesized peptide sequence: IGSVKPTCTY NECRGCRSRCRAEQVPVEGNDPINSAYHYRCICHR, Sangon Biotech, Shanghai, China) was dissolved in 20 mM Tris-HCl, pH 8.8, and 50 mM NaCl and then dialysed (Sangon Biotech,0.5 KD-1 KD) for 1 day at 4□ against 0.5 mM glutathione (reduced and oxidized forms, Macklin) and 200 mML-arginine (meilunbio) at pH 8.0, which were further dialysed three times against 20 mM Tris-HCl, pH 8.8, and 50 mM NaCl for 1.5 days to remove glutathione.

Stomata induction assay

When the first true leaf or cotyledon appeared in *F. bidentis* plants that had germinated in 1/2 MS sterilized solid medium, F*STOMAGEN* peptide was applied on the plants. After the *F. bidentis* plants was further incubated in 1/2 MS liquid medium at 22℃ for 5 days, stomatal number on the abaxial surfaces for the first true leaf was counted under a differential interference contrast microscope (DIC)**.**

Plotting and statistical analysis

Unpaired two-tailed t-test (a=0.05) were performed by GraphPad Prism 7. The linear regressions (a=0.05) were performed by GraphPad Prism 7. In Fig 4, the F test for the intercept and slope from the linear regression analysis were performed by GraphPad Prism 7. Differences between means of multi-groups were assessed with one-way analysis of variance (ANOVA). Duncan's multiple range test was performed using the agricolae package of the R (https://www.r-project.org/) to detect differences between two groups. The *A* and g_s at the saturated light intensity were extracted from (*2*, *52*) and the data describing the correlation between *SD* and expression level of *STOMAGEN* homologs in Arabidopsis, rice and maize (Fig. 4e,f) was digitized from (*35*, *53*) using the OriginPro 2018.

Discussion

C_4 plants have higher water use efficiency and light use efficiency, as result of the combined effect of decreased operating g_s, g_{smax} and a CO_2 concentrating mechanism (Fig 1b, c) (*3, 4, 10*). Comparative studies using plants from different C_4 clades show that lower g_{smax} is due to either a smaller stomatal size (*SS*) for some C_4 clades, or lower stomatal density (*SD*) for other clades (*10*). We collected and analysed *SD* data from literature for a large number of C_3 and C_4 species (*10, 54-60*). The average *SD* on both sides leaf surface of C_3 species was significantly higher than that of C_4 species (Supplementary fig. 1). Recent studies have shown that when the physiological and ecological differences between C_3 and C_4 plants are compared, the phylogenic effect must be considered (*3, 61*), i.e. comparing either stomatal density or size without considering the phylogeny inevitably has the compounded effect of other genetic factors other than photosynthetic types. So here we used the *Flaveria* genus which contains species with close evolutionary distance and intermediate photosynthetic types to examine changes in *SD* and *SS* during C_4 evolution. We showed that, compared to the *SD* of C_3 species, the *SD* of C_4 species decreased (Fig. 1d, e). This decrease in *SD* is due to less stomata generation rather than augmented stomata and epidermal cells (Fig. 1k). In two other closely related Cleomaecae species, *Gynandropsis gynandra* (C_4) also has a lower *SD* than *Tareneya hassleriana* (C_3), consistent with the difference in their g_s (*62*). In contrast, the *SS* as represented by stomatal length was longer in C_4 species compared to C_3 species in *Flaveria* (Fig. 1e, 4a), consistent with previous reports that *SD* negatively correlates with *SS* (*8*, *14*), suggesting that the *SS* is not an important contributor to the decreased g_{smax} and operational g_s in C_4 species.

The lower *SD* in phylogenetically closely related C_4 species compared to C_3 species suggests that, during evolution from C_3 to C_4 species, the *SD* may gradually decrease. This is indeed shown in (Fig 1d, e, f, g,) where with the gradual transition of

photosynthetic type from C_3 to C_3-C_4 (type I), to C_3-C_4 (type II), to C_4-like and to C_4, there is a gradually decrease in *SD*. Usually stomata conductance is significantly higher on the abaxial surface, as shown in maize, broad bean, and wild tomato species (*63-65*). Here we found that there is a highly significant difference in *SD* on the abaxial surface between the C_3 species and the C_4 species (Fig. 1f,g); by comparison, on the adaxial surface, though the difference between *SD* in the C_3 and C_4 species was smaller, C_4 species still had lower *SD* (Supplemental fig 2c, d). All these show that lower *SD* is the determinant of the commonly observed lower g_{smax} and correspondingly higher water use efficiency in C_4 compared to C_3 plants (*2, 66*). Therefore, lower stomatal density could be another major feature of C_4 evolution, besides C_4 enzymes and Kranz anatomy.

The molecular program controlling stomata differentiation has been extensively studied and the core signal transduction pathway is known (*17, 19, 21, 29*). In theory, since *SD* is controlled by a signaling network composed of many interacting components, many options can be used to alter *SD* by transgenic manipulation, as demonstrated previously, e.g. increasing expression of homologs of *EPF1* to reduce *SD* (*67-70*), increasing the expression of *EPF2* to reduce *SD* (*25*)**, and o**ver-expressing *STOMAGEN* to increase *SD* (*26-28*). In fact, these options have been used to improve WUE and drought resistance (*11, 67-70*) or improve photosynthetic efficiency (*13*). Out of these different options to reduce *SD*, here we present results which indicate that a downregulation of the expression *of FSTOMAGEN*, *STOMAGEN*-like genes, have been selected as a molecular switch to reduce *SD* during C_4 evolution in *Flaveria*, which is also the case in monocotyledon (maize and rice) (Fig 4d). The evidence from this study and previous reports show that the role of *STOMAGEN* in controlling *SD* is well conserved between dicotyledons and monocotyledon (*35, 71*). When synthetic F*STOMAGEN* peptide was applied on young developing leaves, we found that similar increases in *SD* were observed between Arabidopsis and *Flaveria* species (Fig. 3i). Furthermore, when the correlations between the expression level of *STOMAGEN* and *SD* was compared between

524 Arabidopsis and rice, or between Arabidopsis and maize, there is non-significant
525 difference for the slope of the correlations (Fig. 4e, f). All these suggest that the
526 declining expression of *STOMAGEN* homologs underlies the observed decrease in *SD*
527 during the evolution of C_4 photosynthesis.

528 Many earlier studies suggest that water limitation might have been a primary
529 selective pressure for evolution of C_4 photosynthesis (*5-7*). In *F. angustifolia*, a type I
530 C_3-C_4 intermediate *Flaveria* species, when grown under outdoor natural light
531 conditions, the *STOMAGEN* expression level, *SD* and g_s were still similar to those in
532 two C_3 *Flaveria* species, i.e. *F.* cronquistii and *F. pringlei* (*2*) (Fig. 1d, 3b), as also the
533 case in *Helliotropin* (*72*). In contrast, the gamma star of *F. angustifolia* was
534 dramatically decreased (*73*) compared to their C_3 ancestors, as a result of an operating
535 CO_2 concentrating mechanism (CCM) of C_2 (*74*). This suggests that during the
536 evolution from C_3 to C_3-C_4 intermediate species, where the movement of GDC from
537 mesophyll cell to bundle sheath cell occurred, the primary evolutionary driving force
538 should be to elevate CO_2 levels around Rubisco, rather than H_2O saving (*75*). After
539 this step, reducing water loss might became crucial. The emergence of C_2 mechanisms
540 can increase leaf photosynthetic CO_2 uptake rate and biomass production, which can
541 in principle create a higher water demand and increased the danger of embolism,
542 especially in the arid and semi-arid areas, in the intermediate species (*4*). This will
543 create an even greater challenge once the complete C_4 photosynthetic metabolism
544 emerged where photosynthetic CO_2 uptake rate and biomass production are further
545 increased. Therefore, decreased *SD* and further increased water use efficiency
546 observed in this study and earlier studies (*2, 52*) should be a required change during
547 the transition from the C_3-C_4 intermediate species and later C_4 species.

548 Many genes control the guard cell developing, i.e. *STOMAGEN*, *EPFs*/*EPFLs*, *ER*
549 (Fig 3A). In principle, any of these genes controlling stomatal patterning can be
550 potentially selected to alter *SD* by regulation of expression during the emergence of
551 C_4 photosynthesis. In fact, these genes have innate mechanisms to alter their
552 expression under different environments, such as low CO_2 (*76*). However, not only in

553 the *Flaveria* genus, but also in the grass family, *STOMAGEN* was shown to be the
554 regulator selected to reduce *SD*. The two specialities of *STOMAGEN* probably have
555 accounted for the phenomenon. First, *STOMAGEN* can regulates the entire molecular
556 process of stomatal development, rather than *EPF1*, *EPF2*, *TMM* and the members of
557 *ERECTA*, which individually only regulate particular phases of the stomatal
558 development (*18*, *19*, *21*, *22*, *24*, *25*). Second, which is potentially more important,
559 *STOMAGEN* is expressed in the mesophyll cell, while all other regulators controlling
560 stomatal development are expressed in the cell of stomatal lineage (*22*, *24-27*).
561 Having a genetic regulator controlling stomatal density in the mesophyll cell, where
562 many of the C_4 related genes are expressed, can enable an easier coordination between
563 stomatal development and C_4 photosynthesis. Future work is still needed to elucidate
564 molecular level coordinating the expression of *STOMAGEN* and C_4 photosynthetic
565 related genes.

566

567 **Reference**

568 1. O. V. Sedelnikova, T. E. Hughes, J. A. Langdale, Understanding the Genetic Basis of C_4 Kranz
569 Anatomy with a View to Engineering C_3 Crops. *Annu Rev Genet* **52**, 249-270 (2018).

570 2. P. J. Vogan, R. F. Sage, Water-use efficiency and nitrogen-use efficiency of C_3-C_4 intermediate
571 species of Flaveria Juss. (Asteraceae). *Plant, cell & environment* **34**, 1415-1430 (2011).

572 3. S. H. H. Taylor, S. P. Rees, M Ripley, B. S. Woodward, F. I. Osborne, C. P., Ecophysiological traits
573 in C_3 and C_4 grasses: a phylogenetically controlled screening experiment. *New Phytol* **185**,
574 780-791 (2010).

575 4. C. P. Osborne, L. Sack, Evolution of C_4 plants: a new hypothesis for an interaction of CO_2 and
576 water relations mediated by plant hydraulics. *Philos Trans R Soc Lond B Biol Sci* **367**, 583-600
577 (2012).

578 5. H. Zhou, B. R. Helliker, M. Huber, A. Dicks, E. Akcay, C_4 photosynthesis and climate through
579 the lens of optimality. *Proc Natl Acad Sci U S A* **115**, 12057-12062 (2018).

580 6. G. Reeves *et al.*, Natural Variation within a Species for Traits Underpinning C_4 Photosynthesis.
581 *Plant physiology* **177**, 504-512 (2018).

582 7. B. P. Williams, I. G. Johnston, S. Covshoff, J. M. Hibberd, Phenotypic landscape inference
583 reveals multiple evolutionary paths to C_4 photosynthesis. *Elife* **2**, e00961 (2013).

584 8. P. J. Franks, P. L. Drake, D. J. Beerling, Plasticity in maximum stomatal conductance
585 constrained by negative correlation between stomatal size and density: an analysis using
586 Eucalyptus globulus. *Plant, cell & environment* **32**, 1737-1748 (2009).

587 9. T. Doheny-Adams, L. Hunt, P. J. Franks, D. J. Beerling, J. E. Gray, Genetic manipulation of
588 stomatal density influences stomatal size, plant growth and tolerance to restricted water
589 supply across a growth carbon dioxide gradient. *Philos Trans R Soc Lond B Biol Sci* **367**,
590 547-555 (2012).

591 10. S. H. Taylor *et al.*, Photosynthetic pathway and ecological adaptation explain stomatal trait
592 diversity amongst grasses. *New Phytol* **193**, 387-396 (2012).

593 11. P. J. Franks, W. Doheny-Adams T, Z. J. Britton-Harper, J. E. Gray, Increasing water-use
594 efficiency directly through genetic manipulation of stomatal density. *New Phytol* **207**,
595 188-195 (2015).

596 12. E. T. Hamanishi, B. R. Thomas, M. M. Campbell, Drought induces alterations in the stomatal
597 development program in Populus. *J Exp Bot* **63**, 4959-4971 (2012).

598 13. Y. Tanaka, S. S. Sugano, T. Shimada, I. Hara-Nishimura, Enhancement of leaf photosynthetic
599 capacity through increased stomatal density in Arabidopsis. *New Phytologist* **198**, 757-764
600 (2013).

601 14. P. J. F. a. D. J. Beerling, Maximum leaf conductance driven by CO_2 effects on stomatal size and
602 density over geologic time. *PNAS* **106**, 10343–10347 (2009).

603 15. S. h. Zhang, X. f. Xu, Y. m. Sun, J. l. Zhang, C. z. Li, Influence of drought hardening on the
604 resistance physiology of potato seedlings under drought stress. *Journal of Integrative*
605 *Agriculture* **17**, 336-347 (2018).

606 16. Peter J. Franks, G. D. Farquhar, The Effect of Exogenous Abscisic Acid on Stomatal
607 Development, Stomatal Mechanics, and Leaf Gas Exchange in Tradescantia virginiana. *Plant*
608 *physiology* **125**, 935–942 (2001).

609 17. L. J. Pillitteri, K. U. Torii, Mechanisms of stomatal development. *Annu Rev Plant Biol* **63**,
610 591-614 (2012).

611 18. N. Zoulias, E. L. Harrison, S. A. Casson, J. E. Gray, Molecular control of stomatal development.
612 *Biochem J* **475**, 441-454 (2018).

19. G. Lin *et al.*, A receptor-like protein acts as a specificity switch for the regulation of stomatal development. *Genes Dev* **31**, 927-938 (2017).

20. E. D. Shpak, J. M. McAbee, L. J. Pillitteri, K. U. Torii, Stomatal patterning and differentiation by synergistic interactions of receptor kinases. *Science* **309**, 290-293 (2005).

21. J. S. Lee *et al.*, Direct interaction of ligand-receptor pairs specifying stomatal patterning. *Genes Dev* **26**, 126-136 (2012).

22. T. Shimada, S. S. Sugano, I. Hara-Nishimura, Positive and negative peptide signals control stomatal density. *Cell Mol Life Sci* **68**, 2081-2088 (2011).

23. A. L. Rychel, K. M. Peterson, K. U. Torii, Plant twitter: ligands under 140 amino acids enforcing stomatal patterning. *J Plant Res* **123**, 275-280 (2010).

24. K. Hara, R. Kajita, K. U. Torii, D. C. Bergmann, T. Kakimoto, The secretory peptide gene EPF1 enforces the stomatal one-cell-spacing rule. *Genes Dev* **21**, 1720-1725 (2007).

25. L. Hunt, J. E. Gray, The signaling peptide EPF2 controls asymmetric cell divisions during stomatal development. *Curr Biol* **19**, 864-869 (2009).

26. S. S. Sugano *et al.*, Stomagen positively regulates stomatal density in Arabidopsis. *Nature* **463**, 241-244 (2010).

27. T. Kondo *et al.*, Stomatal density is controlled by a mesophyll-derived signaling molecule. *Plant Cell Physiol* **51**, 1-8 (2010).

28. L. Hunt, K. J. Bailey, J. E. Gray, The signalling peptide EPFL9 is a positive regulator of stomatal development. *New Phytol* **186**, 609-614 (2010).

29. J. S. Lee *et al.*, Competitive binding of antagonistic peptides fine-tunes stomatal patterning. *Nature* **522**, 439-443 (2015).

30. L. J. Pillitteri, K. U. Torii, Breaking the silence: three bHLH proteins direct cell-fate decisions during stomatal development. *Bioessays* **29**, 861-870 (2007).

31. S. Ohki, M. Takeuchi, M. Mori, The NMR structure of stomagen reveals the basis of stomatal density regulation by plant peptide hormones. *Nat Commun* **2**, 512 (2011).

32. U. Gowik, A. Bräutigam, K. L. Weber, A. P. M. Weber, P. Westhoff, Evolution of C_4 Photosynthesis in the Genus Flaveria: How Many and Which Genes Does It Take to Make C_4? *The Plant Cell* **23**, 2087-2105 (2011).

33. J. Mallmann *et al.*, The role of photorespiration during the evolution of C_4 photosynthesis in the genus Flaveria. *Elife* **3**, e02478 (2014).

644 34. M. Hronkova *et al.*, Light-induced STOMAGEN-mediated stomatal development in
645 Arabidopsis leaves. *J Exp Bot* **66**, 4621-4630 (2015).

646 35. J. Lu *et al.*, Homologous genes of epidermal patterning factor regulate stomatal development
647 in rice. *J Plant Physiol* **234-235**, 18-27 (2019).

648 36. L. Xuxin, The Effects for Stomata Developmental on Arabidopsis by Overexpression of Rice
649 EPFL Family Genes. *Molecular Plant Breeding* **15**, 2042- 2047 (2017).

650 37. J. Y. Zhang, S. B. He, L. Li, H. Q. Yang, Auxin inhibits stomatal development through
651 MONOPTEROS repression of a mobile peptide gene STOMAGEN in mesophyll. *Proc Natl Acad*
652 *Sci U S A* **111**, E3015-3023 (2014).

653 38. Z. Xu, G. Zhou, Responses of leaf stomatal density to water status and its relationship with
654 photosynthesis in a grass. *J Exp Bot* **59**, 3317-3325 (2008).

655 39. M. J. Lyu *et al.*, RNA-Seq based phylogeny recapitulates previous phylogeny of the genus
656 Flaveria (Asteraceae) with some modifications. *BMC Evol Biol* **15**, 116 (2015).

657 40. A. L. Ming-Ju *et al.*, The Coordination and Jumps along C_4 Photosynthesis Evolution in the
658 Genus Flaveria. *bioRxiv*, 460287 (2018).

659 41. K. Billakurthi *et al.*, Transcriptome dynamics in developing leaves from C_3 and C_4 Flaveria
660 species reveal determinants of Kranz anatomy. *bioRxiv*, (2018).

661 42. L. Wang *et al.*, Comparative analyses of C_4 and C_3 photosynthesis in developing leaves of
662 maize and rice. *Nat Biotechnol* **32**, 1158-1165 (2014).

663 43. X. Robert, P. Gouet, Deciphering key features in protein structures with the new ENDscript
664 server. *Nucleic Acids Res* **42**, W320-324 (2014).

665 44. D. R. F. Kyte J, A simple method for displaying the hydropathic character of a protein. *Journal*
666 *of Molecular Biology* **157**, 105-132 (1982).

667 45. X. J. Min, G. Butler, R. Storms, A. Tsang, OrfPredictor: predicting protein-coding regions in
668 EST-derived sequences. *Nucleic acids research* **33**, W677-680 (2005).

669 46. M.-J. A. Lyu *et al.*, The Coordination and Jumps along C4 Photosynthesis Evolution in the
670 Genus Flaveria. *bioRxiv*, 460287 (2018).

671 47. S. A. Shiryev, J. S. Papadopoulos, A. A. Schaffer, R. Agarwala, Improved BLAST searches using
672 longer words for protein seeding. *Bioinformatics* **23**, 2949-2951 (2007).

673 48. R. C. Edgar, MUSCLE: multiple sequence alignment with high accuracy and high throughput.
674 *Nucleic acids research* **32**, 1792-1797 (2004).

675 49. A. Stamatakis, RAxML-VI-HPC: Maximum likelihood-based phylogenetic analyses with
676 thousands of taxa and mixed models. *Bioinformatics* **22**, 2688-2690 (2006).

677 50. J. L. J. a. T. F. Ø. Claus Lindbjerg Andersen, Normalization of real-time quantitative reverse
678 transcription-PCR data a model-based variance estimation approach to identify genes suited
679 for normalization, applied to bladder and colon cancer data sets. *Cancer Res* **64**, 5245-5250
680 (2004).

681 51. D. P. K. Vandesompele J, Pattyn F, Poppe B, Van Roy N, De Paepe A, Speleman F., Accurate
682 normalization of real-time quantitative RT-PCR data by geometric averaging of multiple
683 internal control genes. *Genome Biology* **3**, research0034.0031–0034.0011 (2002).

684 52. D. A. Way, G. G. Katul, S. Manzoni, G. Vico, Increasing water use efficiency along the C_3 to C_4
685 evolutionary pathway: a stomatal optimization perspective. *J Exp Bot* **65**, 3683-3693 (2014).

686 53. Q. Chen, Functional analysis of STOMAGEN-like gene in regulating stomatal development in
687 maize. *Master*, (2017).

688 54. V. S. R. D. a. M. Santakumari, Stomatal characteristics of some dicotyledonous plants in
689 relation to the C_4 and C_3 pathways of photosynthesis. *Plant and cell physiology* **18**, 935-938
690 (1977).

691 55. M. E. K. a. S. A. M. Marc D. Abrams, Relating Wet and Dry Year Ecophysiology to Leaf
692 Structure in Contrasting Temperate Tree Species. *Ecology* **75**, 123-133 (1994).

693 56. C. T. a. D. R. Murray, Effects of Elevated Atmospheric CO_2 Concentration on Leaf Anatomy and
694 Morphology in Panicum Species Representing Different Photosynthetic Modes. *International*
695 *Journal of Plant Sciences* **160**, 1063-1073 (1999).

696 57. A. S. Soares *et al.*, Adaxial/abaxial specification in the regulation of photosynthesis and
697 stomatal opening with respect to light orientation and growth with CO_2 enrichment in the C_4
698 species Paspalum dilatatum. *New Phytologist* **177**, 186-198 (2007).

699 58. I. Gindel, Stomatal Number and Size as Related to Soil Moisture in Tree Xerophytes in Israel
700 *Ecological Society of America* **50**, 263-267 (1968).

701 59. V. S. Pathare, N. Koteyeva, A. B. Cousins, Increased adaxial stomatal density is associated with
702 greater mesophyll surface area exposed to intercellular air spaces and mesophyll
703 conductance in diverse C4 grasses. *The New phytologist* **225**, 169-182 (2019).

704 60. J. A. Cardoso, M. Pineda, L. Jimenez Jde, M. F. Vergara, I. M. Rao, Contrasting strategies to
705 cope with drought conditions by two tropical forage C_4 grasses. *AoB Plants* **7**, plv107 (2015).

706 61. E. J. Edwards, C. J. Still, M. J. Donoghue, The relevance of phylogeny to studies of global
707 change. *Trends Ecol Evol* **22**, 243-249 (2007).

708 62. S. Aubry *et al.*, A Specific Transcriptome Signature for Guard Cells from the C_4 Plant
709 Gynandropsis gynandra. *Plant physiology* **170**, 1345-1357 (2016).

710 63. S. P. Driscoll, A. Prins, E. Olmos, K. J. Kunert, C. H. Foyer, Specification of adaxial and abaxial
711 stomata, epidermal structure and photosynthesis to CO_2 enrichment in maize leaves. *J Exp*
712 *Bot* **57**, 381-390 (2006).

713 64. W.-H. W. Xi-Qing Wang, and Sarah M. Assmann, Differential Responses of Abaxial and Adaxial
714 Guard Cells of Broad Bean to Abscisic Acid and Calcium. *Plant physiology* **118**, 1421–1429
715 (1998).

716 65. C. D. Muir, M. À. Conesa, J. Galmés, Independent evolution of ab- and adaxial stomatal
717 density enables adaptation. *biorxiv*, (2015).

718 66. R. J. Webster *et al.*, High C_3 photosynthetic capacity and high intrinsic water use efficiency
719 underlies the high productivity of the bioenergy grass Arundo donax. *Sci Rep* **6**, 20694 (2016).

720 67. R. S. Caine *et al.*, Rice with reduced stomatal density conserves water and has improved
721 drought tolerance under future climate conditions. *The New phytologist* **221**, 371–384
722 (2018).

723 68. U. Mohammed *et al.*, Rice plants overexpressing OsEPF1 show reduced stomatal density and
724 increased root cortical aerenchyma formation. *Scientific reports* **9**, 5584 (2019).

725 69. J. Dunn *et al.*, Reduced stomatal density in bread wheat leads to increased water-use
726 efficiency. *J Exp Bot* **70**, 4737-4748 (2019).

727 70. J. Hughes *et al.*, Reducing Stomatal Density in Barley Improves Drought Tolerance without
728 Impacting on Yield. *Plant physiology* **174**, 776-787 (2017).

729 71. X. Yin *et al.*, CRISPR-Cas9 and CRISPR-Cpf1 mediated targeting of a stomatal developmental
730 gene EPFL9 in rice. *Plant Cell Rep* **36**, 745-757 (2017).

731 72. P. J. Vogan, M. W. Frohlich, R. F. Sage, The functional significance of C_3-C_4 intermediate traits
732 in Heliotropium L. (Boraginaceae): gas exchange perspectives. *Plant, cell & environment* **30**,
733 1337-1345 (2007).

734 73. J. W. Maurice S. B. Ku, Ziyu Dai, Rick A. Scott, Chun Chu, and Gerald E. Edwards,
735 Photosynthetic and Photorespiratory Characteristics of Flaveria species. *Plant physiology* **96**,
736 518-528 (1991).

74. O. Keerberg, T. Parnik, H. Ivanova, B. Bassuner, H. Bauwe, C_2 photosynthesis generates about 3-fold elevated leaf CO_2 levels in the C_3-C_4 intermediate species Flaveria pubescens. *J Exp Bot* **65**, 3649-3656 (2014).

75. R. F. Sage, T. L. Sage, F. Kocacinar, Photorespiration and the evolution of C_4 photosynthesis. *Annu Rev Plant Biol* **63**, 19-47 (2012).

76. C. B. Engineer *et al.*, Carbonic anhydrases, EPF2 and a novel protease mediate CO_2 control of stomatal development. *Nature* **513**, 246-250 (2014).

Acknowledgements

The work was funded by Strategic Priority Research Program of the Chinese Academy of Sciences (grant number: XDB27020105) and the general program of National Science Foundation of China (31870214). We thank Prof. Rowan F. Sage (University of Toronto) for providing the Flaveria cuttings.

Author contributions

YYZ and XGZ designed the study. YYZ observed and measured the stomatal characteristic. YYZ carried out the molecular experiment and the treatment of synthetic peptides in vivo. GYC guided the treatment of peptides in vivo. Amy MJL analyzed the one kp RNA-seq data. YYZ and XGZ interpreted results and wrote the article.

Competing interests

The authors declare no competing financial interests.

761 Figure Legend

762 Fig 1: Stomatal conductance, density (*SD*) and its patterning.

763 **a**, Stomatal conductance (g_s) responses to net photosynthesis rate (*A*) under saturated
764 light. The circles on the graph indicate larger g_s values in different photosynthetic
765 types (Date from (*2, 52*)). **b**, The average operating g_s and *A* at saturated light. Error
766 bar indicates s.e.m. **c**, G_s responses to *A* at the growth light in two *Flaveria* species (*F.*
767 *Robusta*: rob, *F. bidentis*: bid). **d**, **e**, The difference in *SD* of abaxial surface between
768 species with different photosynthetic types in *Flaveria* genus grown outdoors (**d**) and
769 in greenhouse (**e**). The type I represents C_3-C_4 (type I), and the type II represents
770 C_3-C_4 (type II)**. f**, **g**, The change of *SD* of abaxial surface from C_3 to C_4 in *Flaveria*
771 species grown outdoors (**f**) and in greenhouse (**g**). (n=4, biologically independent
772 replicates). **h**, Correlation between *SD* and g_s under the saturated light. **i,** The
773 photographs of stomatal patterning on abaxial surface in rob, ram and bid. The
774 photographs from the left to right are for rob, ram and bid grown outdoors (top) and in
775 greenhouse (bottom). **j**, **k**, Comparison of guard cell length(*l*) (**j**) and stomatal index
776 (SI) (**k**) between rob, ram, and bid. Different colours represent plants grown outdoors
777 (blue) or in greenhouse (green). *l*, (n=20, biologically independent replicates). *SI*,
778 (n=3, biologically independent replicates). Error bar indicates s.d. Different letters
779 represent statistically significant differences (one-way ANOVA, Duncan's multiple
780 range test (α = 0.05)). The asterisks represent statistically significant differences
781 (P<0.05, t-test, two-tailed distribution, unpaired)

782

783 Fig 2: The Function of *FSTOMAGEN* in controlling the *SD*

784 **a**, Protein conservative analysis of the homologs of FSTOMAGEN in different
785 species. The amino acid regions marked by green line and red line represent the signal
786 peptide and the functional domain of FSTOMAGEN, respectively. Red letters
787 represent conserved amino acids in most species, white letters with red backgrounds

represent amino acid conserved across all species. **b**, Phylogenetic tree for FSTOMAGEN. blue represents dicotyledon and red represents monocotyledon. **c**, The structure of recombinant genes used to transform Arabidopsis. AFSTO represents the recombination of the signal peptide of STOMAGEN from Arabidopsis and the functional domain of FSTOMAGEN from *F.robusta*. FSTO represents the intact STOMAGEN from *F.robusta*. **d**, Photographs showing stomata on a leaf for the wild type Arabidopsis. Scar bar represents 10 um. **e**, Photographs of stomata in a leaf from Arabidopsis with AFSTO over-expressed. Scar bar represents 10 um. The bar graph shows the difference in *SD* between WT and AFSTO overexpression in Arabidopsis. **f**, Photographs of stomata in a leaf from Arabidopsis with FSTO over-expressed. Scar bar represents 10 um. The bar graph shows the difference in *SD* between WT and FSTO overexpression in Arabidopsis. **g**, Photographs of leaf surface taken differential interference contrast microscope showing the increased stomata density in *F. bidentis* (*bid*) leaves with FSTOMAGEN applied. Scale bar represents 20 um. **h**, The stomatal density for *bid* leaves with FSTOMAGEN applied at different concentrations (n=3, biologically independent replicates). **i**, The *SD* in leaves of *bid* and Arabidopsis treated with FSTOMAGEN and STOMAGEN respectively at different concentration. The percentage indicates the percentage increase of *SD* in the treated group compared to that in the untreated group. Error bar indicates s.d. The asterisks represent statistically significant differences ($P<0.05$, t-test, two-tailed distribution, unpaired).

Fig 3: Transcript abundance of stomatal developmental related genes between species with different photosynthetic types in the *Flaveria* genus.

a, A model of the signaling pathway for the stomatal development in Arabidopsis. A protodermal cell (PDC, white) becomes a meristemoid mother cell (MMC, orange), which divides asymmetrically into two daughter cells, with one being a meristemoid (M, red) and the other being a stomatal-lineage ground cell (SLGC). The M cell develops into a guard mother cell (GMC, yellow); the SLGC develops into a

816 pavement cell (PC). The GMC conducts an symmetrical division to produce two
817 equal-sized guard cells (GC, green). EPF1, EPF2 and STOMAGEN competitively
818 bind to ER and TMM, which can deliver a signal to the YDA MAPK cascade. SPCH,
819 MUTE and FAMA ultimately are inactivated through phosphorylation by the YDA
820 MAPK cascade. **b**, Comparison of the transcript abundance of stomatal development
821 related genes between C_3, C_3-C_4, C_4-like and C_4 specie in *Flaveria* genus. J represents
822 samples from the juvenile leaves, M represents samples from mature leaves. C_3, C_3-C_4,
823 C_4-like and C_4 were arranged from the left to right sequentially. **c**, Relative expression
824 levels determined by RT-qPCR and expression level determined by RNA-seq of
825 FSTO (FSTOMAGEN), FEPF1 and FEPF2 in *rob* and *bid* (n=4, biologically
826 independent replicates). **d**, Protein conservative analysis of the homologs of
827 FSTOMAGEN between different species in the *Flaveria* genus. The amino acid
828 regions marked by green line and red line represent the signal peptide and the
829 functional domain of STOMAGEN, respectively. Red letters represent conserved
830 amino acids in most species; white letters with red background represent amino acids
831 conserved across all species. **e**, Expression levels of *FSTOMAGEN* at the different
832 developmental stages of leaves in *rob* and *bid*. **f**, Comparison of the expression levels
833 of *FSTOMAGEN* between different species with different photosynthetic types in
834 *Flaveria* genus. **g,** Comparison of relative expression levels of *FSTOMAGEN* between
835 *rob*, *ram* and *bid*. (n=3, biologically independent replicates). **h**, Combined data show
836 the relation between *SD* (n=4, biologically independent replicates) and expression
837 levels of *FSTOMAGEN* (n≥3, biologically independent replicates). The relative
838 expression in figure **(c)**, **(f)**, **(h)** indicate the measurements with RT-qPCR, and the
839 others was measured with RNA-seq. The geometric means of *EF1a* and *ACT7* were
840 used as the reference in the calculation of expression levels for other genes. Error bars
841 indicate s.d. The asterisks represent statistically significant differences (P<0.05, t-test,
842 two-tailed distribution, unpaired)

843

844 Fig 4, Comparison of stomatal pattern and expression levels of stomatal development
845 related genes between rice (C_3) and maize (C_4).

846 **a**, Stomatal characteristics for rice and maize. *SD*, (n=8, biologically independent
847 replicates); *l*, (n=25, biologically independent replicates); *SI*, (n=3, biologically
848 independent replicates); g_s, (n=8, biologically independent replicates). Error bar
849 indicates s.d. The asterisks represent statistically significant differences (P<0.05, t-test,
850 two-tailed distribution, unpaired). **b**, Photographs of stomatal pattern in rice and
851 maize. Scale bars represent 50 um. **c**, Comparison of transcript abundance of stomatal
852 development related genes between rice and maize. The developmental stages of
853 leaves were divided into 11 and 15 parts in rice and maize, respectively. R represents
854 the leaves of rice, M represents the leaves of maize. **d**, Comparison of the expression
855 levels of *STOMAGEN* homologs between rice and maize. There are two and three
856 paralogs of *STOMAGEN* in rice and maize, respectively. We summed up their
857 expression levels to calculate the overall *STOMAGEN* homologs expression levels in
858 maize and rice. **e**,**f**, Comparison of the differences in correlation between *SD* and
859 relative mRNA levels of the homologs of *STOMAGEN* for Arabidopsis and rice (**e**),
860 Arabidopsis and maize (**f**). *OsSTOMAGEN* represents the homologs of *STOMAGEN*
861 in rice. *ZmSTOMAGEN* represents the homologs of *STOMAGEN* in maize.

862

863 Legends for Supplemental Figures

864 Supplementary fig 1. Comparison of *SD* between C_3 and C_4 species. **a**, Comparison of
865 SD on abaxial surface of leaves between 70 C_3 and 47 C_4 species, with data collected
866 from literature (see details in the discussion section). b, Comparison of *SD* on adaxial
867 surface of leaves between 26 C_3 and 27 C_4 species with data collected from literature
868 (see details in the discussion section). Error bar indicates s.d. The asterisks represent
869 statistically significant differences (P<0.05, t-test, two-tailed distribution, unpaired).

Supplementary fig 2: *SD* on the adaxial surface of leaves in Flaveria. **a**, **b**, The changes of *SD* on the adaxial leaf surface from C_3 to C_4 species in the *Flaveria* genus grown outdoors (**a**) and in greenhouse (**b**). (n=3, biologically independent replicates). **c**, **d**, The difference in *SD* in species with different photosynthetic types grown outdoors (**c**) or in greenhouse (**d**)**.** Different letters represent statistically significant differences (one-way ANOVA, Duncan's multiple range test ($\alpha = 0.05$)).

Supplementary fig 3: *SD* in *rob* (C_3), *ram* (C_3-C_4) and *bid* (C_4) grown from seeds. The *SD* on abaxial (ab) (n=5, biologically independent replicates) and adaxial (ad) (n=4, biologically independent replicates) surfaces were observed in *rob*, *ram* and *bid* grown in greenhouse. Different colours represent different photosynthetic types. Different letters represent statistically significant differences (one-way ANOVA, Duncan's multiple range test ($\alpha = 0.05$)).

Supplementary fig 4: Conservative analysis of amino acid sequences for EPF1 and EPF2. **a**. Comparison of amino acid sequences of homologs of EPF1 between different *Flaveria* species and Arabidopsis. **b**. Comparison of amino acid sequences of homologs of EPF2 between *Flaveria* species and Arabidopsis. White letters with red background represent amino acids conserved across all species. Red letters represent amino acids with similar biochemical property.

Supplementary fig 5: Hydrophobicity analysis of proteins. **a**, the protein of stomagen (left) and the protein of FSTOMAGEN (right). **b**, the protein of EPF1 (left) and the protein of FEPF1 (right). **c**, the protein of EPF2 (left) and the protein of FEPF2 (right).

Supplementary fig 6: Assessment of the stability of expression levels of reference genes. **a**,**b**, Comparison of the stability of expression levels of candidate reference genes in the *Flaveria* species by RNA-seq. **c**, Gel electrophoresis showing the specificity of the primers for candidate reference genes. From left to right, *ACT7*, *EF1a*, *J3*, *PNdO*, *CPN20*, *UBC9*, *GAPDH*, *F2N1.5*, *PSRP4*, *CACMS*, *HEME2*, and *UBQ11*. **d**, The coefficient of variations (CV) for the candidate reference genes. **e**,

The expression stability for candidate reference genes calculated by Genorm. **f**, The expression stability for candidate reference genes calculated by Normfinder.

Supplementary fig 7: The expression levels of stomatal development related genes in *Flaveria* by RNA-seq. Expression levels of stomatal development related genes in species with different photosynthetic types in the *Flaveria* genus.

Supplementary fig 8: Relative expression levels of FSTOMAGEN and *SD* for rob (C_3) under different light conditions. (A) Relative expression levels for FSTOMAGEN under two different light conditions. (B) *SD* under two different light conditions. Natural light: the maximal photosynthetic photon flux density in the greenhouse was about 1300~1400 mmol m^{-2} s^{-1}. Light in the phytotron: 20~100 mmol m^{-2} s^{-1}. Reference gene used to calculate the expression level was *ACT7*. The asterisks represent statistically significant differences ($P<0.05$, t-test, two-tailed distribution, unpaired).

Supplementary fig 9: Relative expression levels of stomata development related genes determined with different reference genes and different primers. **a, b, c,** Quantification with different primers and the same *EF1a* reference gene. Relative expressions shown in **a and b** were determined using the same primer pairs while that in **c** used other primer pairs (See details of the primers used in Table S2). **d,** Relative expression levels determined with the gene *J3* used as the reference gene.

Supplementary fig 10: Transcript abundance of genes in the C_4 cycle and C_4 related transporters. J represents juvenile leaves and M represents mature leaves. Different colours represent species with different photosynthetic types in the *Flaveria* genus. Red colour represents C_3 species, grey colour represents C_3-C_4 species, green colour represents C_4-like species, and blue colour represents C_4 species.

Supplementary fig 11: Alignment of the functional domain of *STOMAGEN* with transcripts from different *Flaveria* species by Blast. From the top to bottom, *F.*

924 *robusta*, *F. pringlei*, *F. angustifolia*, *F. ramosissima*, *F. vaginata*, *F. australasica*, *F.*
925 *bidentis*.

926 Supplementary fig 12: The increase of *SD* in cotyledon of *F. bidentis* (*bid*) with in
927 vitro application of FSTOMAGEN. Photographs of the leaf surface in the untreated
928 (control) and treated bid plants. scale bar, 20 mm.

929

930

931

932

933 Supplementary table 1: Statistics for the mapping of the RNA-seq data of the juvenile
934 and mature leaves in different species from the Flaveria genus.

935 Supplementary table 2: primers used in this study

936

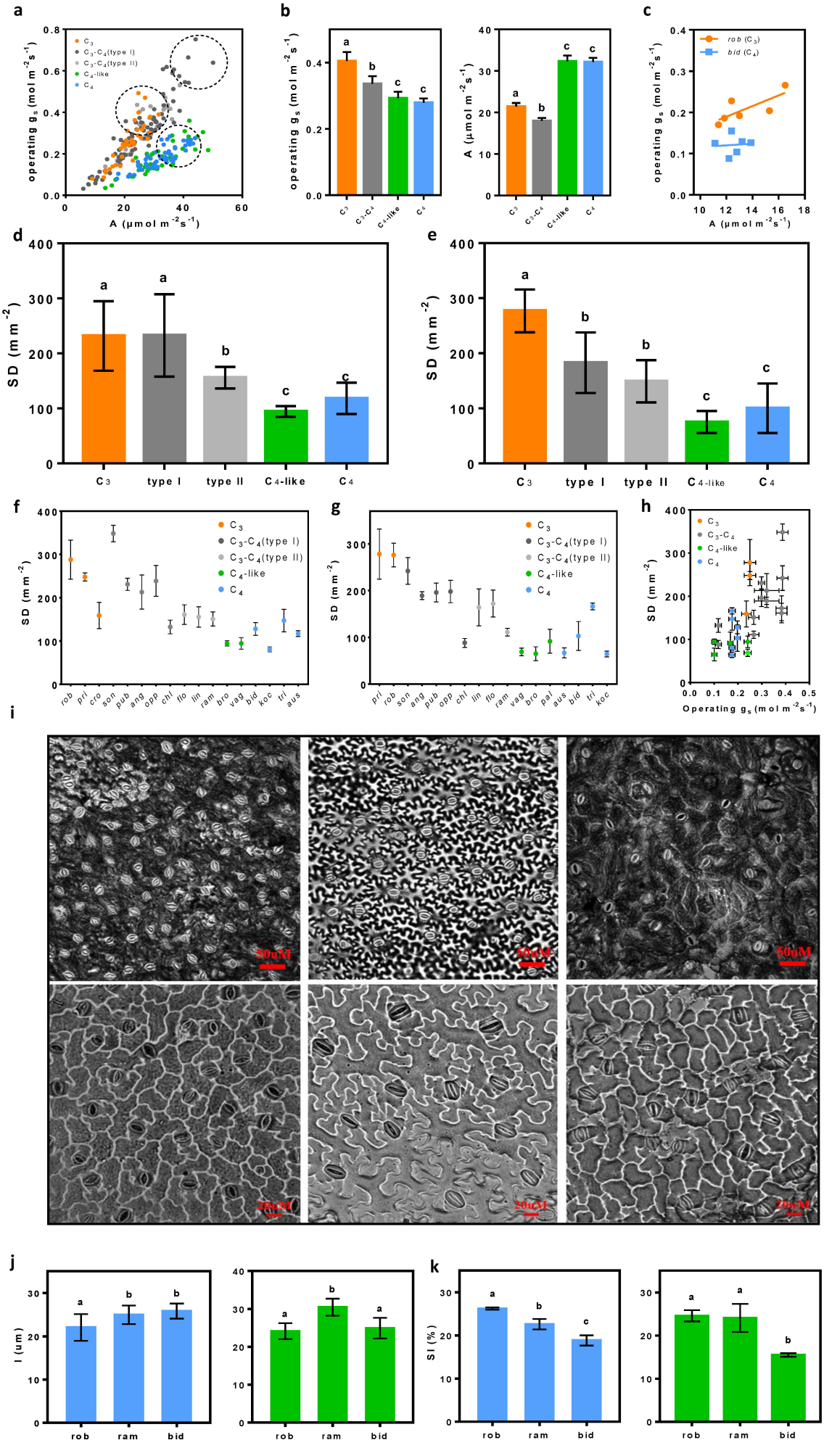

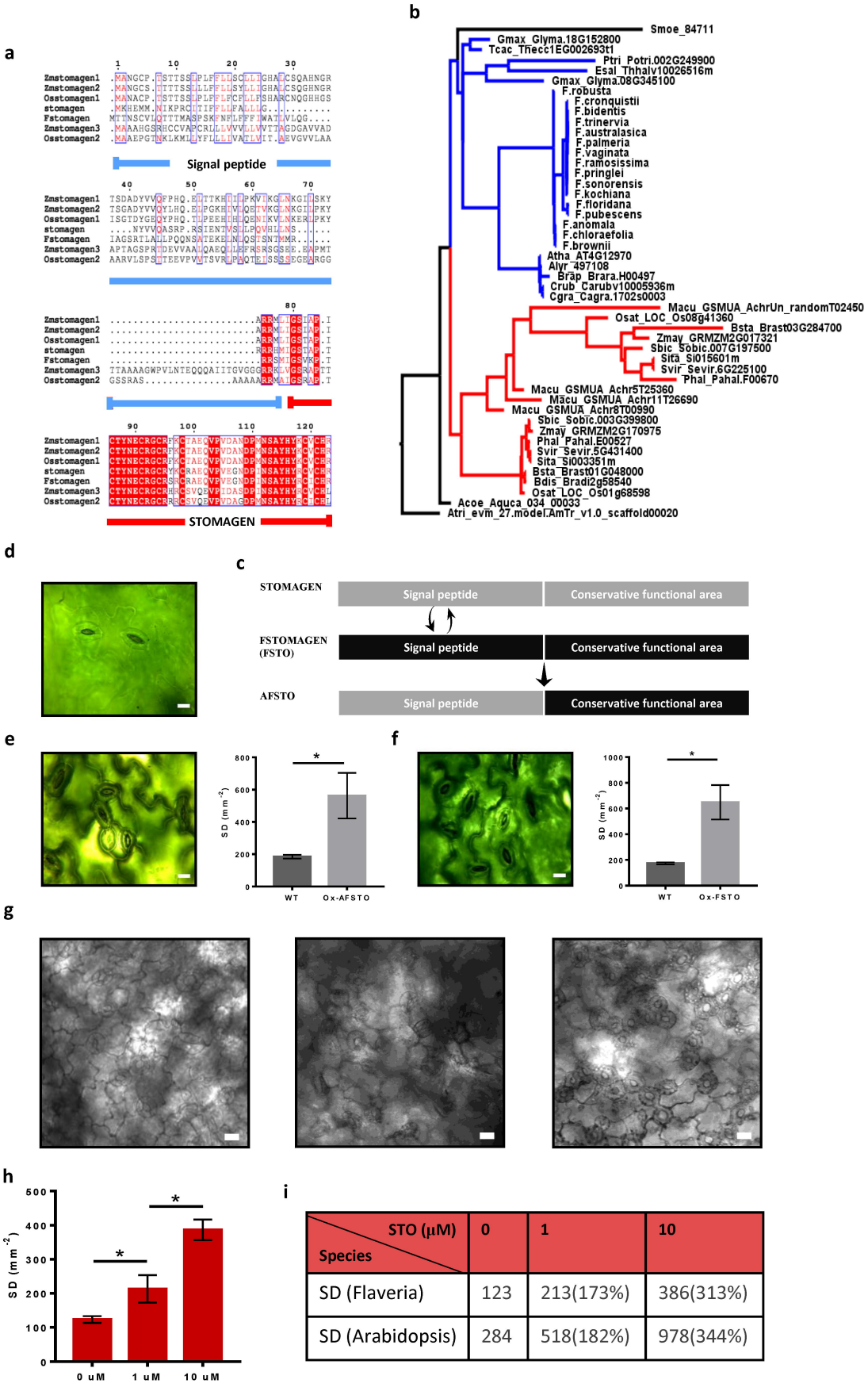

STO (μM) / Species	0	1	10
SD (Flaveria)	123	213(173%)	386(313%)
SD (Arabidopsis)	284	518(182%)	978(344%)

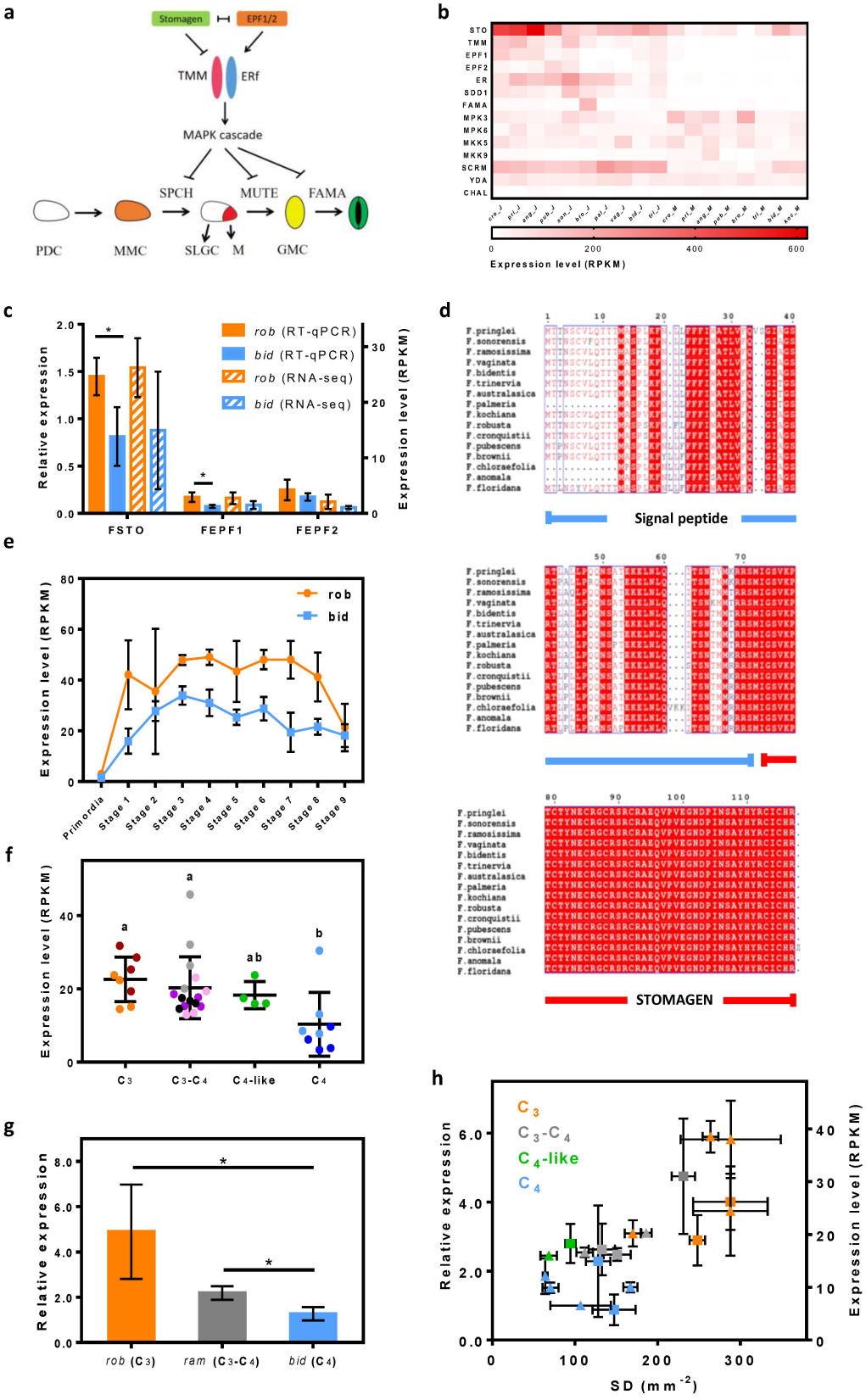

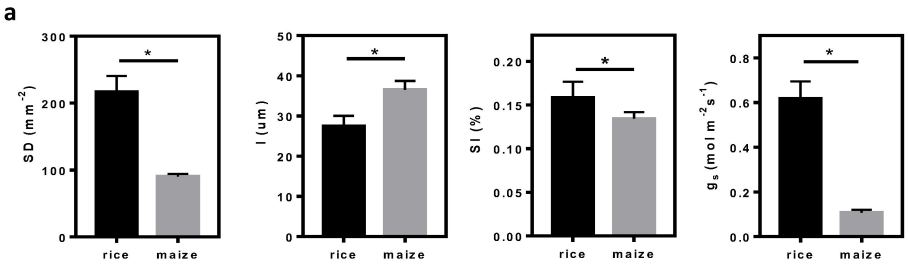

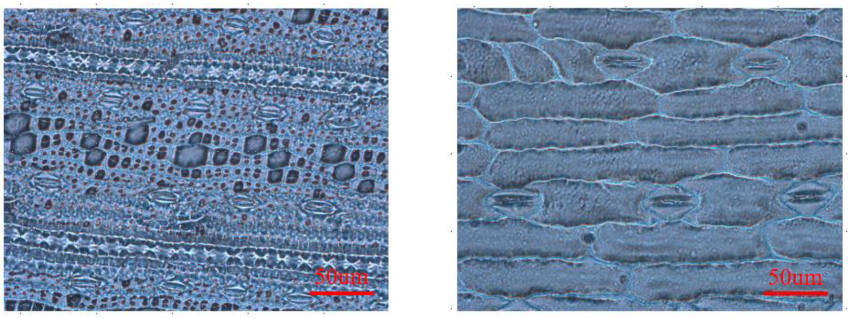

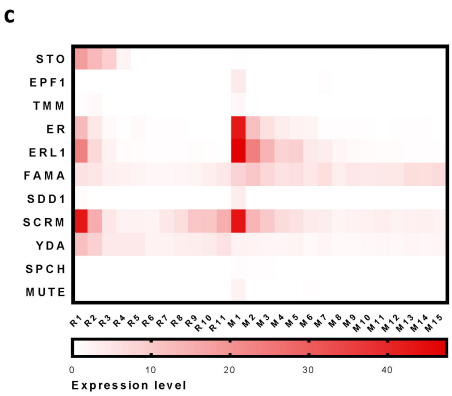

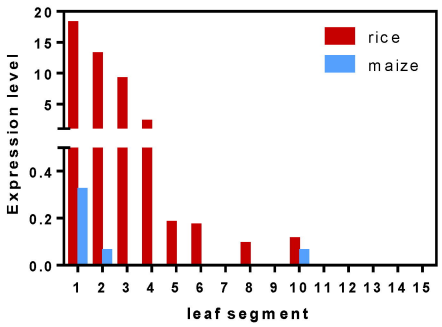

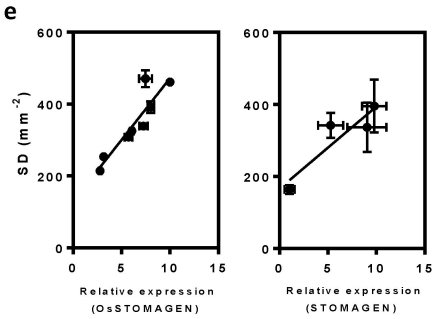

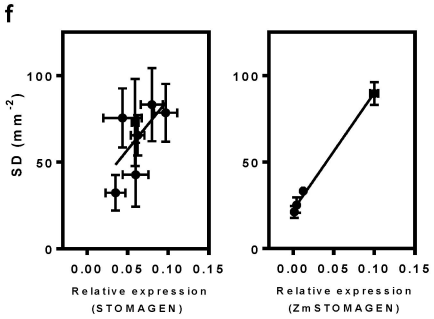

	slope	intercepts
F	1.551	1.656
P	0.2483	0.2303

	slope	intercepts
F	0.07351	0.002883
P	0.7954	0.9587